

Robust sliding mode control of a DFIG based on the SVM strategy

Ibrahim Yaichi¹, Kouddad Elhachemi^{1,2}, Aoumri Mohammed¹

¹Department of Electrical Engineering, Faculty of Science and Technology, LDDI Laboratory, University of Ahmad Draia, Adrar, Algeria

²Department of Telecommunications, Telecommunication and Digital Signal Processing Laboratory, Faculty of Electrical Engineering, University Djillali Liabes, Sidi-Bel-Abbes, Algeria

Article Info

Article history:

Received Mar 11, 2025

Revised Aug 9, 2025

Accepted Sep 2, 2025

Keywords:

Conventional direct-power control

Doubly fed induction generator

Renewable energy

Sliding mode control

Space vector modulation

Wind turbine

ABSTRACT

This paper presents a direct power control (DPC) method for a doubly-fed induction generator (DFIG) used in variable-speed wind power systems, combining sliding mode control (SMC) with space vector modulation (SVM). The proposed SMC-based DPC with SVM (SMC-DPC_SVM) achieves decoupled power control through flux orientation, enhancing performance through the robustness of SMC and the precision of SVM. Simulation results demonstrate the effectiveness of this control strategy. The conventional direct power control (C-DPC) approach delivers fast and robust power response, and a comparative analysis between C-DPC and the proposed SMC-DPC_SVM strategy highlights the advantages of the latter. Robustness was evaluated under varying machine parameters, confirming system stability. The proposed control method was implemented and validated using MATLAB/Simulink, achieving a total harmonic distortion (THD) of less than 5%, indicating high-quality power delivery to the electrical grid.

This is an open access article under the [CC BY-SA](#) license.



Corresponding Author:

Ibrahim Yaichi

Department of Electrical Engineering, Faculty of science and technology, Universitas Ahmad Draia

Adrar 01000, Algeria

Email: ibrahimyaichi@gmail.com

1. INTRODUCTION

Currently, most wind turbines utilize doubly-fed induction generators (DFIGs) due to their numerous advantages, such as variable speed operation ($\pm 30\%$ around synchronous speed), independent control of active and reactive power, reduced mechanical stress and noise, improved power quality, and lower costs [1]. However, DFIGs face several challenges, including parametric uncertainties caused by factors like heating and magnetic saturation, as well as disturbances due to rotor speed fluctuations. These factors can lead to suboptimal system performance, highlighting the need for robust and high-performance control strategies [2]. To address this, we have adopted a direct power control (DPC) approach enhanced by sliding mode control (SMC) and space vector modulation (SMC-DPC_SVM).

Though the doubly-fed induction machine (DFIM) was first introduced in 1899 [2], it is not a new structure, but rather a renewed supply method [3]. In wind turbine applications, where DFIGs are widely used, the rotor speed is adjusted based on wind speed, enabling both sub-synchronous and super-synchronous operation. Variable speed capability allows wind turbines to extract maximum power across a wide range of wind conditions [4]. Initially, the control of electric machines was handled using direct torque control (DTC), which manages stator flux and electromagnetic torque without modulation blocks [3], [4]. This was later extended to DPC by [5], [6], primarily for grid-connected rectifiers, where the focus shifted to controlling instantaneous active and reactive power.

This study focuses on the modeling and control of the DFIG system, including the converter and turbine, using a combination of SVM and SMC within a DPC framework. Our approach introduces a novel hybrid strategy (SMC-DPC_SVM) that aims to enhance the performance of conventional direct power control (C-DPC) by reducing ripples in active/reactive power and minimizing the THD in stator and rotor currents. Simulation results demonstrate that the SMC-DPC_SVM strategy significantly outperforms the conventional C-DPC. The THD in both stator and rotor currents remains below the 5% threshold set by the IEEE Standards Association, confirming the effectiveness and efficiency of the proposed method [6]. Comparative simulations of C-DPC and SMC-DPC_SVM under various step changes in active and reactive power further validate these findings.

2. DESCRIPTION OF A WIND ENERGY CONVERSION SYSTEM

The wind energy conversion system depicted in Figure 1 consists of several key components: a wind turbine that captures kinetic energy from the wind, a gearbox (or speed multiplier) that increases the rotational speed to match the operational requirements of the generator, a doubly-fed induction generator (DFIG) that facilitates variable-speed operation and efficient energy conversion, and a power electronic converter that regulates the power flow between the generator and the electrical grid, ensuring stable and controlled energy output.

The turbine converts the kinetic energy of the wind into mechanical energy. The total kinetic power available to the wind turbine can be mathematically represented as (1):

$$P = \frac{1}{2} \rho S v^3 \quad (1)$$

In wind turbines, the power extraction coefficient C_p , which is a function of both wind speed and the turbine's rotational speed, typically varies between 0.35 and 0.59 [7]. The DFIG subsequently converts the mechanical energy into electrical energy. Power converters are utilized to optimize the transfer of the generated energy to the electrical grid, ensuring maximum efficiency under varying wind conditions [8], [9].

$$C_p(\beta, \lambda) = (0.5 - 0.0167(\beta - 2)) \sin \left[\frac{\pi(\lambda + 0.1)}{18.5 - 0.3(\beta + 2)} \right] - 0.00184(\lambda - 3)(\beta - 2) \quad (2)$$

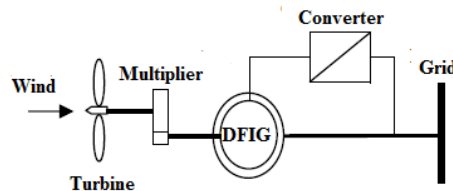


Figure 1. Schematic representation of a wind energy conversion system

3. MODELING AND VECTOR CONTROL OF THE DFIG

The modeling of the DFIG is conducted within the park reference frame. The following set of equations represents the comprehensive mathematical model of the generator.

$$\begin{cases} V_{ds} = R_s I_{ds} + \frac{d\phi_{ds}}{dt} - \omega_s \phi_{qs} \\ V_{qs} = R_s I_{qs} + \frac{d\phi_{qs}}{dt} + \omega_s \phi_{ds} \\ V_{dr} = R_r I_{dr} + \frac{d\phi_{dr}}{dt} - (\omega_s - \omega_r) \phi_{qr} \\ V_{qr} = R_r I_{qr} + \frac{d\phi_{qr}}{dt} + (\omega_s - \omega_r) \phi_{dr} \end{cases}, \quad (3)$$

$$\begin{cases} \phi_{ds} = L_s I_{ds} + M I_{dr} \\ \phi_{qs} = L_s I_{qs} + M I_{qr} \\ \phi_{dr} = L_r I_{dr} + M I_{ds} \\ \phi_{qr} = L_r I_{qr} + M I_{qs} \end{cases} \quad (4)$$

$$J \frac{d\Omega}{dt} = C_{em} - C_r - f\Omega \quad (5)$$

$$V_{dr} = R_r I_{dr} + \left(L_r - \frac{M^2}{L_s}\right) \frac{dI_{dr}}{dt} - g \left(L_r - \frac{M^2}{L_s}\right) \omega_s I_{qr} \quad (6)$$

$$V_{qr} = R_r I_{qr} + \left(L_r - \frac{M^2}{L_s}\right) \frac{dI_{qr}}{dt} + g \left(L_r - \frac{M^2}{L_s}\right) \omega_s I_{dr} + g \frac{M V_s}{L_s} \quad (7)$$

4. SLIDING MODE CONTROL

SMC belongs to the class of variable structure control systems, which operate by switching between multiple control laws. SMC is valued for its key advantages: high precision, rapid dynamic response, inherent stability, ease of design and implementation, and strong robustness against both internal and external parameter variations [10], [11].

a) Choice of the switching surface

Consider a nonlinear system represented in the following form:

$$\begin{cases} \dot{X} = f(X, t) + g(X, t) u(X, t) \\ X \in \mathbb{R}^n, u \in \mathbb{R} \end{cases} \quad (8)$$

Where $f(X, t)$, $g(X, t)$ are two continuous and uncertain nonlinear functions are supposed to be bounded. We take the general equation form proposed in [12] to determine the sliding surface:

$$S(X) = \left(\frac{d}{dt} + \lambda\right)^{n-1} e \quad (9)$$

$$e = X^d - X \quad (10)$$

$$X = [x, \dot{x}, \dots, x^{n-1}]^T, X^d = [x^d, \dot{x}^d, \ddot{x}^d, \dots]^T \quad (11)$$

e : Adjustment error in the controlled variable, λ : positive coefficient, n : system order, X^d : desired size, X : The state variable representing the quantity ordered.

b) Condition ensuring convergence

The condition of convergence is defined by the Lyapunov equation [11], it makes the surface attractive and invariant according to:

$$S(X) \dot{S}(X) \leq 0 \quad (12)$$

c) Control calculation

The control algorithm is characterized by the following relationship:

$$u = u^{eq} + u^n \quad (13)$$

u : order size, u^{eq} = equivalent control quantity, u^n = control switching term:

$$u^n = u^{\max} \text{sat}(S(X)/\emptyset) \quad (14)$$

$$\text{sat}(S(X)/\emptyset) = \begin{cases} \sin(s) & \text{if } |s| > \emptyset \\ s/\emptyset & \text{if } |s| < \emptyset \end{cases} \quad (15)$$

$\text{sat}(S(X)/\emptyset)$: saturation function, \emptyset : threshold width of the saturation function. The equivalent control is a continuous function designed to keep the system's state constrained to the sliding surface $S = 0$. It is derived based on the surface invariance conditions: $S = 0$ and $\dot{S} = 0$. From a physical perspective, the equivalent control represents the average value of the control input u . However, this control alone does not guarantee that the system trajectories will reach the sliding surface. Therefore, the control input u is composed of two parts: the equivalent control and a discontinuous component (3), which ensures convergence to the sliding surface and maintains the system in the sliding mode.

$$u = u^{eq} + u^n \text{ with } u^n = -\text{asign}(S) \quad (16)$$

5. DIRECT POWER CONTROL STRATEGY

5.1. Conventional DPC of the DFIG

The core principle of DPC involves choosing a sequence of switching commands (Sa, Sb, Sc) for the semiconductors from a predefined switching table. This selection is based on the errors between the reference and actual values of active and reactive power, which are processed through two hysteresis comparators generating digital outputs Hp and Hq, respectively. Additionally, the choice depends on the sector (zone) where the rotor flux vector is located [13], [14].

5.2. Estimation of active and reactive powers

Rather than directly measuring the power transmitted through the line, this method involves monitoring the rotor currents to indirectly estimate the stator's active and reactive power components, denoted as Ps and Qs, respectively. By analyzing the rotor current signals, it becomes possible to infer the electromagnetic behavior within the stator windings, thereby enabling more responsive and earlier control of power exchange at the stator side. This approach enhances dynamic performance and has been validated in prior studies [15], [16].

$$\begin{cases} P_s = -\frac{3}{2} \frac{L_m}{\sigma L_s L_r} V_s \varphi_{r\beta} \\ Q_s = \frac{3}{2} \left(\frac{V_s}{\sigma L_s} \varphi_s - \frac{V_s L_m}{\sigma L_s L_r} \varphi_{r\alpha} \right) \end{cases} \quad (17)$$

Where:

$$\begin{cases} \varphi_{r\alpha} = \sigma L_r i_{r\alpha} + \frac{L_m}{L_s} \varphi_s \\ \varphi_{r\beta} = \sigma L_r i_{r\beta} \\ |\vec{\varphi}_s| = \frac{|\vec{V}_s|}{\omega_s} \\ \sigma = 1 - \frac{L_m^2}{L_s L_r} \end{cases} \quad (18)$$

By defining the angle δ between the stator and rotor flux vectors, the expressions for Ps and Qs can be written as:

$$\begin{cases} P_s = -\frac{3}{2} \frac{L_m}{\sigma L_s L_r} \omega_s |\varphi_s| |\varphi_r| \sin \delta \\ Q_s = \frac{3}{2} \frac{\omega_s}{\sigma L_s} |\varphi_s| \left(\frac{L_m}{L_r} |\varphi_r| \cos \delta - |\varphi_s| \right) \end{cases} \quad (19)$$

$$\begin{cases} \frac{dP_s}{dt} = -\frac{3}{2} \frac{L_m}{\sigma L_s L_r} \omega_s |\varphi_s| \frac{d|\varphi_r| \sin \delta}{dt} \\ \frac{dQ_s}{dt} = \frac{3}{2} \frac{L_m \omega_s}{\sigma L_s L_r} |\varphi_s| \frac{d(|\varphi_r| \cos \delta)}{dt} \end{cases} \quad (20)$$

6. SMC-DPC_SVM of the DFIG

6.1. SMC of the DFIG

To regulate the power, a relative degree of $n=1$ is considered. The control surface expressions for the active and reactive power are given by (21) and (22) [17], [18]:

$$S(P) = P_{s-ref} - P_s \quad (21)$$

$$S(Q) = Q_{s-ref} - Q_s \quad (22)$$

During the convergence phase, in order to satisfy the condition $S(P)\dot{S}(P) \leq 0$, we impose:

$$\dot{S}(P) = -V_s \frac{M}{\sigma L_s L_r} V_{qr}^n \quad (23)$$

Hence, the switching term is defined as:

$$V_{qr}^n = KV_{qr} \text{sat}(S(P)) \quad (24)$$

To verify the system stability condition, the parameter KV_{qr} must be strictly positive. To prevent the reference voltage V_{qr} from exceeding its limits, it is often beneficial to include a voltage limiter, which is defined as (25) [19]:

$$V_{qr}^{\text{lim}} = V_{qr}^{\text{max}} \text{sat}(P) \quad (25)$$

During the convergence phase, to ensure the condition $S(Q)\dot{S}(Q) \leq 0$ is met, we set:

$$\dot{S}(Q) = -V_s \frac{M}{\sigma L_s L_r} V_{dr}^n \quad (26)$$

Consequently, the switching term is expressed as:

$$V_{dr}^n = KV_{dr} \text{sat}(S(Q)) \quad (27)$$

To ensure system stability, the parameter KV_{dr} must be positive. To prevent the reference voltage V_{dr} from exceeding its limits, it is often helpful to include a voltage limiter defined as (28):

$$V_{dr}^{\text{lim}} = V_{dr}^{\text{max}} \text{sat}(Q) \quad (28)$$

6.2. SMC-DPC based on the SVM

In this approach, the active and reactive powers are regulated using two sliding mode controllers (SMCs) integrated with the SVM algorithm, thereby obviating the need for switching tables and hysteresis controllers. The SVM technique utilizes a digital algorithm to generate a switching sequence for the inverter switches, resulting in an output voltage vector that closely approximates the reference voltage vector [20], [21]. A representation of the voltage vector is presented in Figure 2. The sector is identified based on the position of the vector V_{r_ref} within the complex plane (α - β), where the phase angle θ of the vector is defined as follows [23]:

$$\theta = \arctan \left(\frac{V_{ref(\beta)}}{V_{ref(\alpha)}} \right) \quad (34)$$

Table 1 determines the sector Z (i) with (i = 1, ..., 6) for the different angles θ .

Figure 3 presents the schematic diagram of the proposed control architecture, referred to as SMC-DPC_SVM, designed for application in DFIGs. The control system integrates two independent sliding mode controllers: one responsible for regulating the stator active power and the other for managing the stator reactive power. These controllers operate in coordination with a space vector modulation (SVM) unit, which ensures the generation of optimal switching signals for the power converter. This architecture aims to achieve robust and precise power control under varying operating conditions while reducing switching losses and enhancing the dynamic response of the system.

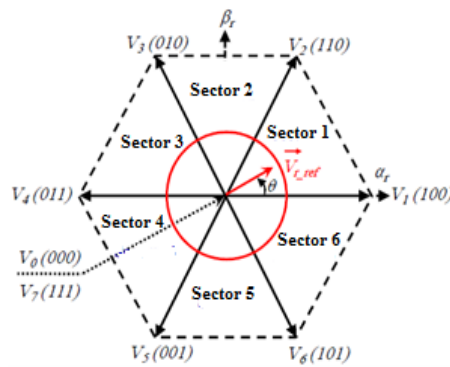


Figure 2. Representation of voltage vectors in the reference (α , β) coordinate frame [22]

Table 1. Sector identification

θ	$0 \leq \theta \leq \frac{\pi}{3}$	$\frac{\pi}{3} \leq \theta \leq 2\frac{\pi}{3}$	$2\frac{\pi}{3} \leq \theta \leq \pi$	$\pi \leq \theta \leq 4\frac{\pi}{3}$	$4\frac{\pi}{3} \leq \theta \leq 5\frac{\pi}{3}$	$5\frac{\pi}{3} \leq \theta \leq 2\pi$
Z	Sector1	Sector2	Sector3	Sector4	Sector5	Sector6

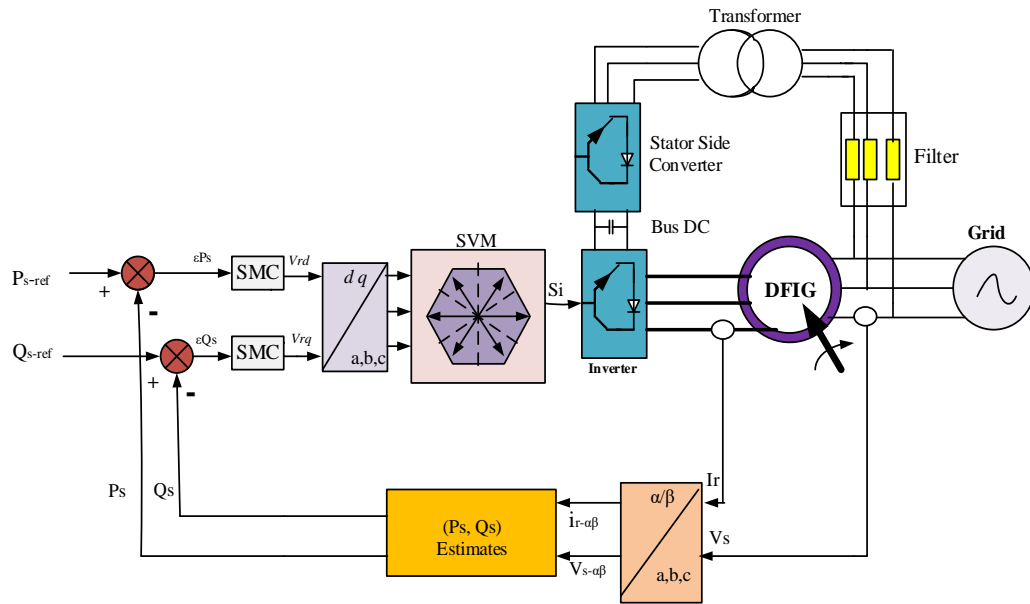


Figure 3. Schematic diagram of DFIG-based SMC-DPC_SVM

7. SIMULATION RESULTS

Both control strategies, C-DPC and the proposed SMC-DPC-SVM, are simulated and evaluated in terms of their reference tracking accuracy, harmonic distortion in the stator currents, and robustness to variations in machine parameters.

7.1. Reference tracking test

The simulation results are presented in the following figures, which illustrate the dynamic performance of the proposed control system under various operating conditions. The simulations were conducted using MATLAB/Simulink, a widely used platform for modeling, simulating, and analyzing dynamic systems. This environment enables accurate representation of the system components and control algorithms, allowing for comprehensive evaluation of the control strategy's effectiveness.

7.2. Robustness test

In order to test the robustness of the C-DPC and SMC-DPC_SVM control, we will study the influence of parametric variations (rotor and stator resistance and inductances). The simulation results show that the SMC-DPC_SVM command is the most efficient in terms of the minimization of the active power and reactive power pulsations as well as the stator current harmonics, compared to the conventional C-DPC command. On the other hand, it can be seen from Figures 4 and 5. The comparison of the differences in the reactive and active powers of the two control strategies, C-DPC and SMC-DPC_SVM, of the DFIG. The results indicate that the SMC-DPC_SVM control strategy is more effective in minimizing the ripple in both active and reactive powers compared to the conventional C-DPC method. Furthermore, the stator and rotor current waveforms, as illustrated in Figures 6 and 7, exhibit nearly sinusoidal shapes with reduced ripple content, reflecting an improved quality of the power delivered to the grid.

The SMC-DPC_SVM control reduces THD (harmonic distortion rate) down to 0.34% compared to C-DPC, where THD is 0.77% by alleviating the chattering phenomenon as shown in Figures 8 and 9. The latter is less than 5% which means a good quality of energy supplied to the electrical networks [24], [25]. Finally, the robustness test results, as shown in Figure 10, show that the SMC-DPC_SVM is more robust compared to C-DPC in the presence of parametric variations of the DFIG. These results allow us to conclude that the SMC-DPC_SVM control is the most efficient in reducing the ripple of active and reactive powers compared to the conventional C-DPC control.

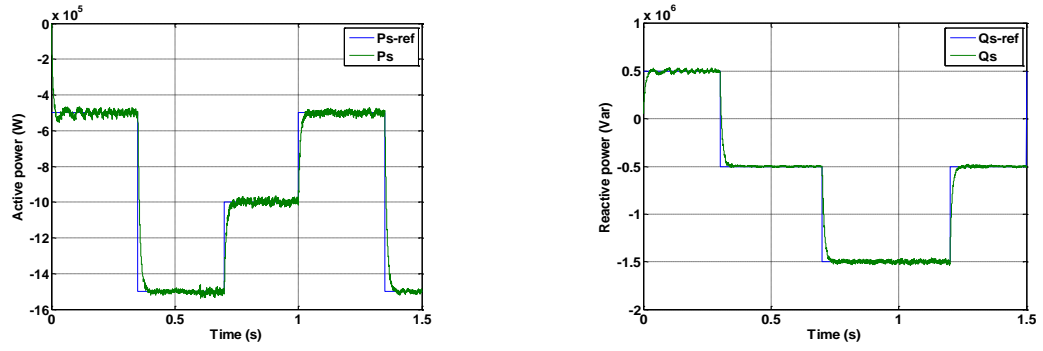


Figure 4. Active and reactive power (C-DPC)

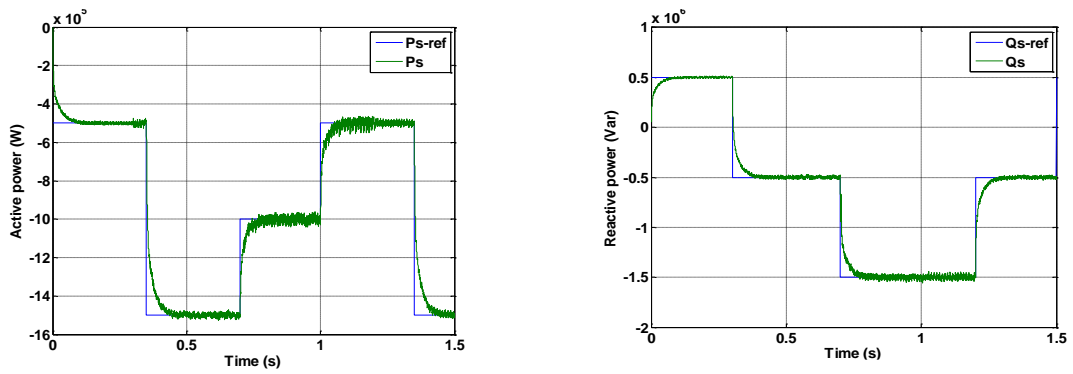


Figure 5. Active and reactive power (SMC-DPC-SVM)

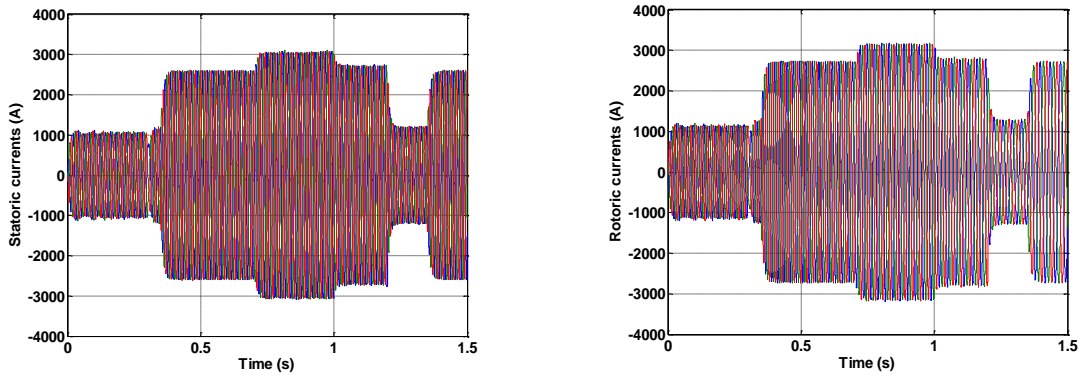


Figure 6. Rotor and stator currents (C-DPC)

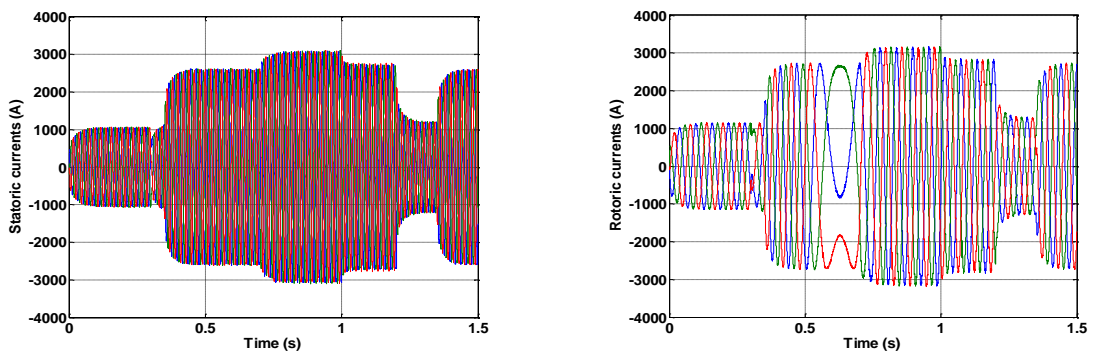


Figure 7. Rotor and stator currents (SMC-DPC-SVM)

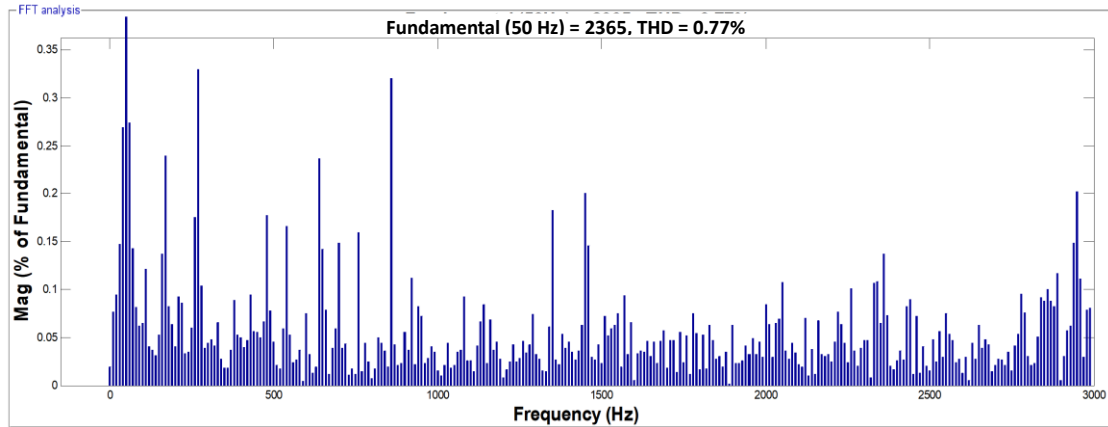


Figure 8. Spectrum harmonic (C-DPC)

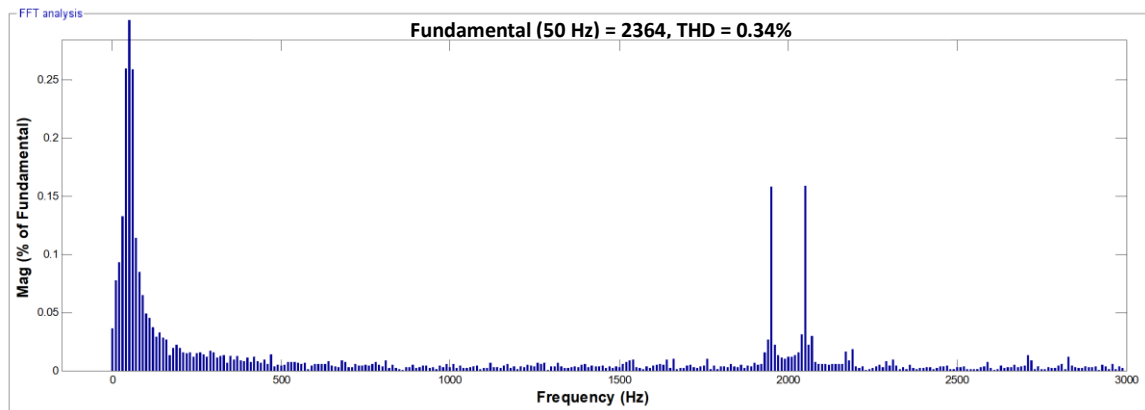


Figure 9. Spectrum harmonic (SMC-DPC_SVM)

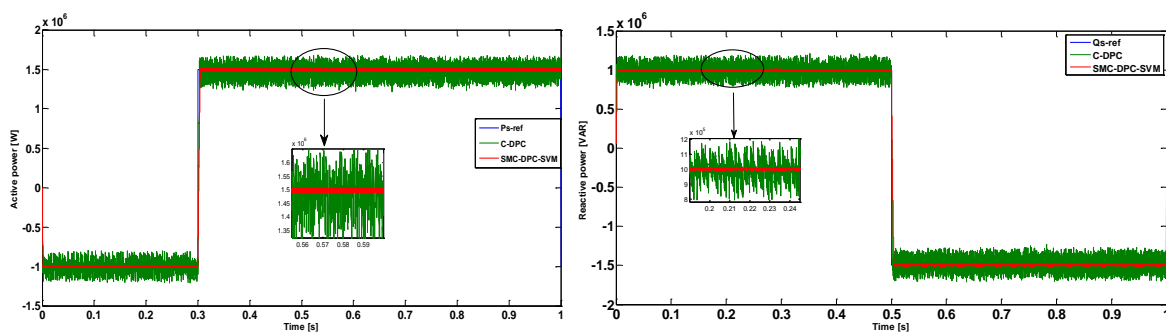


Figure 10. Active and reactive power [C-DPC, SMC-DPC_SVM] (robustness test)

8. CONCLUSION

This paper presents an SMC-DPC_SVM control scheme for a grid-connected DFIG system, implemented on a 1.5 MW wind turbine. The proposed control strategy regulates the active and reactive power exchanged between the doubly fed induction generator and the electrical grid in wind energy conversion systems. By combining the benefits of vector control and conventional DPC, the SMC-DPC_SVM approach effectively addresses power and current fluctuations generated by the DFIG. It achieves precise power decoupling and significantly reduces chattering, even under variations in machine parameters. Therefore, this robust control method emerges as a highly promising solution for devices utilizing DFIGs, such as wind energy conversion systems.

FUNDING INFORMATION

Authors state no funding involved.

AUTHOR CONTRIBUTIONS STATEMENT

This journal uses the Contributor Roles Taxonomy (CRediT) to recognize individual author contributions, reduce authorship disputes, and facilitate collaboration.

Name of Author	C	M	So	Va	Fo	I	R	D	O	E	Vi	Su	P	Fu
Ibrahim Yaichi	✓	✓	✓	✓	✓	✓		✓	✓	✓			✓	
Kouddad Elhachemi	✓	✓	✓	✓	✓	✓		✓	✓	✓	✓	✓		
Aoumri Mohammed	✓	✓	✓	✓	✓	✓	✓			✓	✓		✓	✓

C : **C**onceptualization

M : **M**ethodology

So : **S**oftware

Va : **V**alidation

Fo : **F**ormal analysis

I : **I**nterpretation

R : **R**esources

D : **D**ata Curation

O : **O**riginal Draft

E : **E**diting

Vi : **V**isualization

Su : **S**upervision

P : **P**roject administration

Fu : **F**unding acquisition

CONFLICT OF INTEREST STATEMENT

Authors state no conflict of interest.

DATA AVAILABILITY

Data availability is not applicable to this paper as no new data were created or analyzed in this study.




REFERENCES

- [1] K. F. Sayeh, S. Tamalouzt, D. Ziane, A. Bekhiti, and Y. Belkhier, "Utilizing fuzzy logic control and neural networks based on artificial intelligence techniques to improve power quality in doubly fed induction generator-based wind turbine system," *International Journal of Energy Research*, vol. 2025, no. 1, Jan. 2025, doi: 10.1155/er/5985904.
- [2] K. F. sayeh *et al.*, "Fuzzy logic-enhanced direct power control for wind turbines with doubly fed induction generators," *Results in Engineering*, vol. 24, p. 103557, Dec. 2024, doi: 10.1016/j.rineng.2024.103557.
- [3] K. Ouari and Y. Belkhier, "Model predictive direct torque algorithm for coordinated electrical grid operation of wind energy conversion system-based doubly fed induction generator," *International Journal of Modelling and Simulation*, pp. 1–14, Jun. 2024, doi: 10.1080/02286203.2024.2371680.
- [4] Y. Sahri *et al.*, "Effectiveness analysis of twelve sectors of DTC based on a newly modified switching table implemented on a wind turbine DFIG system under variable wind velocity," *Ain Shams Engineering Journal*, vol. 14, no. 11, p. 102221, Nov. 2023, doi: 10.1016/j.asej.2023.102221.
- [5] T. Noguchi, H. Tomiki, S. Kondo, and I. Takahashi, "Direct power control of PWM converter without power-source voltage sensors," *IEEE Transactions on Industry Applications*, vol. 34, no. 3, pp. 473–479, 1998, doi: 10.1109/28.673716.
- [6] M. Malinowski, M. P. Kazmierkowski, S. Hansen, F. Blaabjerg, and G. D. Marques, "Virtual-flux-based direct power control of three-phase pwm rectifiers," *IEEE Transactions on Industry Applications*, vol. 37, no. 4, pp. 1019–1027, 2001, doi: 10.1109/28.936392.
- [7] M. Rapin and J. M. Noël, *Energie eolienne: principes, etudes de cas*, vol. 33. Paris: Dunod, 2010.
- [8] E. G. Shehata, "Sliding mode direct power control of rsc for DFIGs driven by variable speed wind turbines," *Alexandria Engineering Journal*, vol. 54, no. 4, pp. 1067–1075, Dec. 2015, doi: 10.1016/j.aej.2015.06.006.
- [9] H. S. Ko, G. G. Yoon, N. H. Kyung, and W. P. Hong, "Modeling and control of DFIG-based variable-speed wind-turbine," *Electric Power Systems Research*, vol. 78, no. 11, pp. 1841–1849, Nov. 2008, doi: 10.1016/j.epsr.2008.02.018.
- [10] S. A. E. M. Ardjoun, M. Abid, A. G. Aissaoui, and A. Tahour, "A robust sliding mode control applied to the double-fed induction machine," *Istanbul University - Journal of Electrical and Electronics Engineering*, vol. 12, no. 1, pp. 1445–1451, 2012.
- [11] H. Abouobaida and M. Cherkaoui, "Modelling and control of doubly fed induction (DFIG) wind energy conversion system," *Journal of Electrical Engineering*, vol. 15, no. 1, 2015.
- [12] H. Shariatpanah, R. Fadaeinedjad, and M. Rashidinejad, "A new model for pMSG-based wind turbine with yaw control," *IEEE Transactions on Energy Conversion*, vol. 28, no. 4, pp. 929–937, 2013, doi: 10.1109/TEC.2013.2281814.
- [13] I. Yaichi, A. Semmah, P. Wira, and Y. Djeriri, "Super-twisting sliding mode control of a doubly-fed induction generator based on the svm strategy," *Periodica Polytechnica Electrical Engineering And Computer Science*, vol. 63, no. 3, pp. 178–190, Jun. 2019, doi: 10.3311/PPee.13726.
- [14] A. Mouldia, "DTC-SVM and DPC control strategies applied to a DFIG used for wind energy production (in French)," Doctoral dissertation, Ecole Nationale Polytechnique, Alger, 2014.
- [15] Y. Miloud and A. Draou, "Fuzzy logic speed control of an indirect field-oriented induction machine drive," in *IECON Proceedings (Industrial Electronics Conference)*, Denver, USA, Nov. 2001, pp. 2111–2116. doi: 10.1109/iecon.2001.975618.
- [16] E. G. Shehata, "Sliding mode direct power control of RSC for DFIGs driven by variable speed wind turbines," *Alexandria Engineering Journal*, vol. 54, no. 4, pp. 1067–1075, Dec. 2015, doi: 10.1016/j.aej.2015.06.006.




- [17] C. Wei, W. Qiao, and Y. Zhao, "Sliding-mode observer-based sensor less direct power control of DFIGs for wind power applications," in *2015 IEEE Power & Energy Society General Meeting, IEEE*, Jul. 2015, pp. 1–5. doi: 10.1109/PESGM.2015.7286356.
- [18] I. Yaichi, A. Semmah, M. Djilaila, A. Harrouz, S. Mansouri, and Y. Bakou, "Modelling and control of doubly fed induction machine, application for a wind turbine system," in *Proceedings of 2016 International Renewable and Sustainable Energy Conference, IRSEC 2016*, Nov. 2017, pp. 450–455. doi: 10.1109/IRSEC.2016.7983953.
- [19] Y. Djeriri, A. Meroufel, A. Massoum, and Z. Boudjema, "A comparative study between field-oriented control strategy and direct power control strategy for DFIG," *Journal of Electrical Engineering*, vol. 14, no. 2, pp. 159–167, 2014.
- [20] Y. Yang, R. Hunag, Y. P. Yu, and S. Wang, "Direct torque control of permanent magnet synchronous motor based on space vector modulation control," in *2016 IEEE 8th International Power Electronics and Motion Control Conference, IPEMC-ECCE Asia 2016*, May 2016, pp. 1818–1821. doi: 10.1109/IPEMC.2016.7512570.
- [21] X. Wang, Z. Wang, M. Cheng, and Y. Hu, "Remedial strategies of t-npc three-level asymmetric six-phase pmsm drives based on svm-dtc," *IEEE Transactions on Industrial Electronics*, vol. 64, no. 9, pp. 6841–6853, Sep. 2017, doi: 10.1109/TIE.2017.2682796.
- [22] A. H. Abosh, Z. Q. Zhu, and Y. Ren, "Reduction of torque and flux ripples in space vector modulation-based direct torque control of asymmetric permanent magnet synchronous machine," *IEEE Transactions on Power Electronics*, vol. 32, no. 4, pp. 2976–2986, Apr. 2017, doi: 10.1109/TPEL.2016.2581026.
- [23] G. Abad, M. Á. Rodríguez, and J. Poza, "Predictive direct power control of the doubly fed induction machine with reduced power ripple at low constant switching frequency," in *IEEE International Symposium on Industrial Electronics, IEEE*, Jun. 2007, pp. 1119–1124. doi: 10.1109/ISIE.2007.4374755.
- [24] Yaichi, A. Semmah, and P. Wira, "Control of doubly fed induction generator with maximum power point tracking for variable speed wind energy conversion systems," *Period. Polytech. Electr. Eng. Comput. Sci.*, vol. 64, no. 1, pp. 87–96, 2020.
- [25] A. Bouyekni, R. Taleb, Z. Boudjema, and H. Kahal, "A second-order continuous sliding mode based on DPC for wind-turbine-driven DFIG," *Elektrotehniski Vestnik/Electrotechnical Review*, vol. 85, no. 1–2, pp. 29–36, 2018.

BIOGRAPHIES OF AUTHORS






Ibrahim Yaichi    was born in 1987 in Adrar, Algeria. He received the Engineer degree in Electrical Engineering from the University of Sidi-Bel-Abbes, Algeria, in 2011, and the magister degree from Mustafa Stambouli, Mascara, Algeria, in 2015. He received the Doctorate degree in Electrical Engineering from the University of Sidi Bel Abbess (Algeria) in 2021. He is a permanent researcher of renewable energy in the Renewable Energy Research Unit in the Saharan environment, Adrar (Algeria). He can be contacted at email: ibrahimyaichi@gmail.com.



Kouddad Elhachemi    is a doctor at the Telecommunication and Digital Signal Processing Laboratory, University of Sidi Bel Abbes, Algeria, by nationality, born in 1990 in Adrar. He obtained a Bachelor's degree in Electrical Engineering in 2014 from the University of Sidi Bel Abbes. He then completed a Master's degree in Telecommunication Systems from the same university in 2016. He received a doctorate in telecommunication systems from the University of Sidi Bel Abbess (Algeria) in 2022. He is a permanent researcher in optical telecommunications at the Djillali Liabes University, Sidi Bel Abbes (Algeria). He can be contacted at email: kouddad20@hotmail.fr.



Aoumri Mohammed    is a Ph.D. student at Laboratoire de Développement Durable et Informatique (LDDI), University of Adrar, Algeria. Algerian by nationality, born in 1996 in Adrar. He obtained a Bachelor's degree in Electrical Engineering in 2018 from the University of ADRAR. He then completed a master's degree in Electrical Control from the same university in 2022. He started his Ph.D. studies in electrical machines specialization in 2022 at the same university. His current research interests focus on renewable energy, electrical power systems, adaptive control systems, and control systems using artificial intelligence techniques (neural networks and fuzzy logic). He can be contacted at email: aoumri.moha@univ-adrar.edu.dz.